CHAPTER IV

GENERATION AND ANALYSES OF COX17-DEFICIENT MICE

IV-1. INTRODUCTION

In the previous chapters (CHAPTER II and III), I have presented about the genomic structure and the transcriptional regulation of *COX17* gene. The mouse *COX17* is a single gene which spans ~6 kb, consists of three exons, and maps to the center of chromosome 16 (Takahashi *et al.*, 2001). I also showed that transcription factors Sp1 and NRF-1 (nuclear respiration factor-1) drive the basal transcription of this gene (Takahashi *et al.*, 2002). The transcriptional mechanism of *COX17* is similar to that of other COX subunits which indirectly implies that the Cox17p peptide is also involved in cellular respiration (Scarpulla, 2002). Since my goal is to determine the physiological function of Cox17p in the mammalian system, I tried to generate mice carrying a null mutation for *COX17* and analyze them.

Here, I show the genetic evidence that *COX17* is required for the transport of copper into the mitochondria and CCO activity. Several specific deficiencies of CCO in humans have been known to date, with most cases being associated with severe neonatal or infantile lactic acidosis and early death. For example, patients with a fatal cardioencephalomyopathy or hypertrophic cardiomyopathy, marked by a severe CCO deficiency, have been shown to harbor mutations in the *SCO2* gene which is a related CCO assembly gene and believed to collaborate with Cox17p (Jaksch *et al.*, 2000; Jaksch *et al.*, 2001; Papadopoulou *et al.*, 1999). The *COX17* deficient mouse was embryonic lethal and the fact is consistent with the previous clinical evidences such as the case of *SCO2* mutation. Furthermore, I show here that Cox17p is not only indispensable for the cellular respiration but is also essential for embryonic growth and development. I also demonstrate a marked reduction in CCO activity in 6.5-day (E6.5) viable embryos, indicating that the oxidative phosphorylation-independent embryogenesis progressed up to this stage. Most

recently, gene disruption of *CTR1*, a high-affinity copper transporter on the plasma membrane, was also reported to result in embryonic death (Kuo, *et al.*, 2001; Lee, *et al.*, 2001). The relationship between this molecule and Cox17p is also discussed in the last of this chapter.

IV-2. MATERIALS AND METHODS

IV-2-1. Materials

129SvJ Embryonic stem (ES) cells and green fluorescence protein (GFP) gene were kindly provided by Dr. T. Baba. Neomycin resistance gene (*neo*) was purchased from Stratagene (CA, USA). C57BL/6 mice were purchased from CLEA JAPAN (Tokyo, Japan). Sephadex G-25 column was purchased from Amersham Biosciences (Tokyo, Japan). All reagents for culture of ES cells were purchased from GIBCO BRL (NY, USA). Anti-COX I, II, and IV monoclonal antibodies and Alexa fluor 488 anti-mouse IgG were purchased from Molecular probes (OR, USA). Meyer's hematoxylin, eosin, 3,3-diaminobenzidine (DAB), cytochrome c (from horse heart), catalase, nitro blue tetrazolium (NBT), sodium lactate and β-nicotinamide adenine dinucleotide (β -NAD, from yeast) were purchased from Sigma (Tokyo, Japan). All other materials used in this chapter were obtained as described in CHAPTER II-2-1 or III-2-1.

IV-2-2. Targeted disruption of *COX17* gene

IV-2-2-1. Plasmid construction

The *COX17* genomic clones were isolated from a 129/SvJ mouse genomic library as previously described in CHAPTER II. I replaced a 2.7-kb *Sac* I-*Hin* dIII fragment containing part of the first exon (5' end of ORF) up to the 3'-end of the second exon with green fluorescence protein (GFP) (with the

Nco I site fused with the first ATG of *COX17*) and the *neo* (opposite direction) gene. GFP and *neo* were driven under the control of the endogenous *COX17* promoter and CMV promoter, respectively. Introduction of a negative selection marker, the herpes simplex virus thymidine kinase gene, at the 3' end of the construct (opposite direction) enabled the use of a positive and negative selection scheme (Monsour *et al.*, 1988). The targeting vector was linearized at a unique Sal I site before transfection into 129/SvJ ES cells.

IV-2-2-2. Cell culture

Embryonic stem cells (ES cells) were cultured in the presence of neomycin-resistant embryonic fibroblasts (EF cells) in Dulbecco's modified Eagle's medium (DMEM) supplemented with 15 % fetal calf serum (FCS), 0.1 mM non-essential amino acids, 0.1 mM β-mercaptoethanol, 20 mM L-glutamine, 30 μM adenosine, 30 μM guanocine, 30 μM cytidine, 30 μM uridine, 10 μM thymidine, and 1000U/ml leukemia inhibitory factor (LIF). Cells were incubated in a humidified atmosphere of 5 % CO_2 and 95 % air at 37℃.

IV-2-2-3. Transfection and analysis of ES cells

Sal I-linearized targeting vector (25 μg) was electroporated into 129/SvJ mouse ES cells. Cells were selected with G418 after 24 hr. Double-resistant colonies were screened by PCR using a *COX17* primer set (5'-ATGGCTTC-GAAGTCGGGG-3'; 5'-CCTTTCAGGGTCTTGTGC-3') and a *neo* primer set (5'-CCATTGCTCAGCGGTGCTG-3'; 5'-GCCAAGGAGATGG-TATGTATGTATG-3'). PCR-positive clones were confirmed by Southern blot using probes A and B shown in Fig. IV-1.

IV-2-2-4. Generation of chimeric and *COX17*-deficient mice

Five targeted clones were injected into C57BL/6 blastocysts; two

produced germ-line chimeras. Chimeras were mated with C57BL/6 females, and all further analyses were performed on a mixed (129/SvJ x C57BL/B6) background. Two lines exhibited the same mutant phenotype. Offspring were genotyped by PCR as described above.

IV-2-3. RNA analysis

Total RNAs were extracted from organs and embryos as described in CHAPTER III. Total RNAs (20 μg each) were denatured with glyoxal, electrophoresed through a 1.5% agarose gel, and blotted on to a GeenScreen Plus membrane as recommended by the manufacture. The blot was hybridized with a ^{32}P -labeled cDNA probe specific for mouse Cox17p (as described in CHAPTER II) at 60 ℃, and a final wash was carried out at 60 ℃ in 2× NaCl/Cit/1% SDS for 30 min twice. Hybridized blots were imaged and analyzed by using a BAS 5000. Samples were normalized by determination of the amount of mouse mouse glyceroaldehyde-3-phosphate dehydrogenase (GAPDH; GenBank accession no. M32599).

IV-2-4. Biochemical analysis of CCO

Mouse tissues were homogenized in 0.25 M sucrose buffer containing 3 mg/ml (final) digitonin. CCO activity was measured by the method of Capaldi and co-workers (Capaldi *et al.*, 1995) with slight modifications. Horse cytochrome c was reduced with ascorbate and then desalted using a Sephadex G-25 column. The concentration of the reduced substrate was determined spectrophotometrically at a wavelength of 550 nm. All spectrophotometrical measurements were performed using a UV-160A spectrophotometer (Shimadzu).

IV-2-5. Histological staining

Fresh frozen sections (8 μm) of embryos in decidua were prepared with cryostat CM30503 (Leica).

IV-2-5-1. Hematoxylin and eosin staining

Sections were stained with Meyer' s hematoxylin and 0.6% eosin Y in distilled water.

IV-2-5-2. Cytochrome c oxidase activity

Sections were incubated in 5 mM phosphate buffer (pH 7.4) containing 0.1% 3,3-diaminobenzidine (DAB), 0.1% cytochrome c (from horse heart) and 0.02% catalase for 1 hr at 37℃.

IV-2-5-3. Succinate dehydrogenase activity

Sections were incubated in 0.1 M phosphate buffer (pH 7.4) containing 0.1 M sodium succinate and 0.1% nitro blue tetrazolium (NBT) for 1 hr at 37℃.

IV-2-5-4. Lactate dehydrogenase activity

Sections were incubated in 0.2 M Tris-HCl buffer (pH 7.0) containing 2.5% sodium lactate, 0.1% NBT and 0.04 % β-nicotinamide adenine dinucleotide (β -NAD, from yeast) for 30 min at 37℃.

IV-2-6. Immunohistochemistry

Fresh frozen sections (8 μm) prepared as described IV-2-4 immunostained with anti-COXI, II, and IV monoclonal antibodies and then Alexa fluor 488 anti-mouse IgG as secondary antibody by standard procedures (Sciacco and Bonilla, 1996).

IV-3. RESULTS

IV-3-1. Targeted disruption of the *COX17* gene

To disrupt the gene, a targeting vector was constructed in which the *COX17* sequence coding from half of exon 1 to the end of exon 2 was replaced by a green fluorescence protein (GFP)–neomycin cassette (Fig. IV-1). This construct was electroporated into 129SvJ embryonic stem (ES) cells, and correctly targeted ES cells were discerned by Southern blot (Fig. IV-2. A) and PCR analyses (Fig. IV-2. B). The homologous recombinants were injected into blastocysts, and the disrupted *COX17* allele transmitted through the germ line to the next generation. F1 heterozygotes were generated by crossing the chimeras with C57BL/6J females.

IV-3-2. Analysis of *COX17* (+/-) mice

The heterozygous mice appeared to be healthy; they were fertile and of normal size. Northern blotting experiments demonstrated that the *COX17* (+/-) mice expressed ~50% the levels of the Cox17p mRNA of wild-type littermates in the brain, heart, kidney, and skeletal muscle (Fig. IV-3. A). Then, we asked whether any effect on CCO activity could be discerned in the heterozygous animals. While CCO activity was reduced in the brains of the heterozygotes by less than 20 % compared with wild-type littermates, no significant difference was observed in the kidney or skeletal muscle (Fig. IV-4). The perturbations in the levels of Cox17p expression, through the inactivation of one *COX17* allele, do not give pronounced affects in the most of tissues without brain.

IV-3-3. Mice lacking *COX17* die during early embryogenesis

Progenies from intercrosses of these heterozygous mice were genotyped 3 weeks after birth (Table IV-1). The ratio of wild-type to heterozygous littermates was 1.0:1.9. This indicated an embryonic lethal phenotype associated with the *COX17* (-/-) genotype. The stage of embryonic death associated with *COX17* loss of function was investigated by determining the genotypes of embryos between E14 and E10. No homozygous *COX17* (-/-) fetuses were found in this term and the ratio of *COX17* (+/+) to *COX17* (+/-) fetuses was 1.0:2.5. Therefore, we performed PCR to genotype pregastrulation stage embryos. Among 41 fetuses isolated at E6.5, nine were *COX17* (+/+), 22 were *COX17* (+/-), and ten were *COX17* (-/-). This ratio is maintained until E8.5 and in close agreement with the expected ratio for Mendelian inheritance (Table IV-1). However, no homozygous mutant embryos were found beyond E8.5. Thus, homozygous null mutations in *COX17* result in lethality between E8.5 and E10. Northern blotting experiments demonstrated that the *COX17* mRNAs were already expressed in these stages (Fig. IV-3. B).

IV-3-4. Morphology and histochemistry of *COX17* (-/-) embryos

The development of the embryo appeared to advance by E6.5 in all progenies of heterozygous matings (Fig. IV-5). Whereas wild-type littermates at E7.5 proceeded gastrulation, *COX17* (-/-) embryos were severely retarded, and appeared more fragile upon dissection of the decidua (Fig. IV-6). At E8.5, the wild-type embryos further proceeded to form a neural tube and somite (Fig. IV-5 and IV-6); the embryonic region was smaller than the extraembryonic region and the embryonic cavity had shrunk in mutant embryos (Fig. IV-6). Furthermore, at E8.5, many embryonic cells

became smaller than those of the wild-type littermates and condensed nuclei were observed in some of these cells (Fig. IV-9).

IV-3-5. Oxidative phosphorylation and glycolysis of *COX17* (-/-) embryos

Whereas the wild-type embryos isolated at E6.5 retained the CCO activity, *COX17* (-/-) embryos isolated at the same stage have already shown severe reduction in the CCO activity in embryonic and extraembryonic tissues. This defect was also observed in later stages (Fig. IV-7).

The CCO-defective phenotype of *COX17* (-/-) indicates the possibility that gene disruption of the *COX17* allele may affect not only the transport of copper to the mitochondria but also other steps of oxidative phosphorylation. COXI, COXII and COXIV are subunits of complex IV (CCO), and SDH participates in the oxidative phosphorylation as complex II. No differences in SDH activity between *COX17* (-/-) mice and wild-type littermates were observed (Fig. IV-8, SDH). The immunoreactivity of the COXI, II and IV subunits also appeared normal (Fig. IV-8, COXI, II, IV). Furthermore, strong signals for LDH, the terminal enzyme of glycolysis, were detected in all types of embryo (Fig. IV-8, LDH).

IV-4. DISCUSSION

In this chapter, I showed that the defect of cellular respiration and peri-gastrulation lethality associated with targeted disruption of the *COX17* gene in mice.

The targeting vector was designed in which the *COX17* sequence coding from half of exon 1 to the end of exon 2 was replaced by a GFP –neomycin cassette (Fig. IV-1). GFP was expected to be expressed by the endogenous *COX17* promoter enabling us to analyze the expression pattern of

Cox17p. The heterozygous pups grew normally and appeared to be healthy; they were fertile and of normal size. Contrary to the expectation, the basal expression level of *COX17* was too low to detect the expression of GFP in *COX17* (+/-) tissues. Since CCO activity was reduced by less than 20% in the total brain homogenates from *COX17* (+/-) as compared with wild-type littermates, no significant difference were observed in the other tissue (Fig. IV-4). Based on these observations I concluded that the heterozygosity of *COX17* is phenotypically normal. On the contrary, homozygous disruption of the mouse *COX17* gene leads to CCO deficiency, followed by embryonic death (Fig. IV-7). Since W303DCOX17 strains, a deletion mutant of the yCox17p gene, exhibit a specific CCO deficiency in the presence of nonfermentable carbon sources (Glerum *et al.*, 1996), the phenotype of *COX17* (-/-) embryo is similar with that of the yeast *cox17* null mutant.

In addition to the CCO deficiency, severe developmental defects were observed in the *COX17* (-/-) mutant. The phenotype of *COX17* (-/-) embryo is strikingly similar to that of *CTR1* (-/-) in its lethality around the time of gastrulation (Kuo *et al.*, 2001, Lee *et al.*, 2001). Furthermore, an incomplete embryonic cavity and apoptosis in the embryonic region were common to both *COX17* (-/-) and *CTR1* (-/-) embryos (Fig. IV-6 and IV-9). To date, three different peptides, Atox1, CCS and Cox17p, that transport Cu from CTR1 to three different cellular locations have been identified (CHAPTER I). The targeted disruption of the *ATOX1* and *CCS* genes were already performed and both phenotypes in the embryogenesis were normal; *ATOX1* (-/-) was died perinatally (Hamaza *et al.*, 2001) and *CCS* (-/-) was born as a mature infant (Wong *et al.*, 2000). To the best of my knowledge, Cox17p is a prominent candidate as the copper chaperone involved in the early embryogenesis downstream of CTR1 to date.

The most exciting finding is that a normal embryogenesis of *COX17* (-/-) proceeds until at least E6.5 without CCO activity (Fig. IV-5). A severe reduction in CCO activity was also observed in the case of fatal infantile cardioencephalomyopathy with mutations in *SCO2* (Jaksch *et al.*, 2000; Jaksch *et al.*, 2001; Papadopoulou *et al.*, 1999). Human *SCO2* is required for the assembly of COX subunits I and II into the holoprotein, and for the incorporation of copper to CCO (Jaksch *et al.*, 2001). The histochemistry of muscles from patients with cardioencephalomyopathy revealed reductions in CCO activity in all fibers, but SDH activity appeared normal. Immunohistochemistry showed a severe reduction in the number of mitochondrial DNA-encoded COX I and II subunits (Papadopoulou *et al.*, 1999). The major difference between *COX17* (-/-) and the *SCO2* mutant is the existence of these subunits in the mitochondria. Since immunoreactivity for the subunits was confirmed to exist in the *COX17* (-/-) embryo (Fig. IV-8, COXI, II and IV), I speculated that the CCO deficiency was solely caused by failure of copper transport to the mitochondria. This severe defect is observed at E6.5 when cell division proceeds vigorously in embryonic and extraembryonic regions. Since the activity of the terminal glycolytic enzyme LDH was detected not only in the wild-type and heterozygote but also in homozygote (Fig. IV-8, LDH), glycolysis occurred normally at this stage. Although this finding seemed controversial, if one considers the minimal energy (generated by glycolysis) requirement in early embryogenesis, CCO activation may not be required.

On the other hand, why did the normal development of *COX17* (-/-) embryos stop after E6.5? Since many atrophied cells and nuclear condensation (Fig. IV-9) were observed in the *COX17* (-/-) embryo, a possible mechanism of developmental retardation is hypothesized as follows: CCO inactivation by disruption of the *COX17* allele might cause embryonic cell

death. As gastrulation does not proceed without the migration of mesodermal cells, apoptosis of these cells due to CCO deficiency will lead to developmental retardation and embryonic death. In general, formation of the brain (which rises from the neural tube), heart, skeletal muscle and kidney (which are all derived from the mesoderm) starts after gastrulation. Since Cox17p mRNA is also highly expressed in these organs (Kako *et al.*, 2000), the mesodermal cell death in *COX17* (-/-) may be associated with this expression pattern. The finding of embryonic lethality in *COX17* mutants may provide an explanation for the lack of obvious candidates of human diseases attributable to the severe CCO deficiency in the heart, brain and skeletal muscles, such as the case of *SCO2* mutation. Such significant function of this Cox17p in cellular respiration may be the basis for treating some fatal cardioencephalomyopathy or hypertrophic cardiomyopathy.

Table IV-1. Genotypes of progeny from heterozygous matings

Stage	No. of progeny (%) with genotype:			Total no.
	+/+	+/–	–/–	
Newborn*	32 (34)	61 (66)	0 (0)	93
E13-14	10 (29)	25 (71)	0 (0)	35
E10	4 (29)	10 (71)	0 (0)	14
E8.5	4 (22)	10 (56)	2 (22)	18
E7.5	6 (30)	9 (45)	5 (25)	20
E6.5	9 (22)	22 (54)	10 (24)	41

* DNA was isolated from 2 to 4-week-old animals.

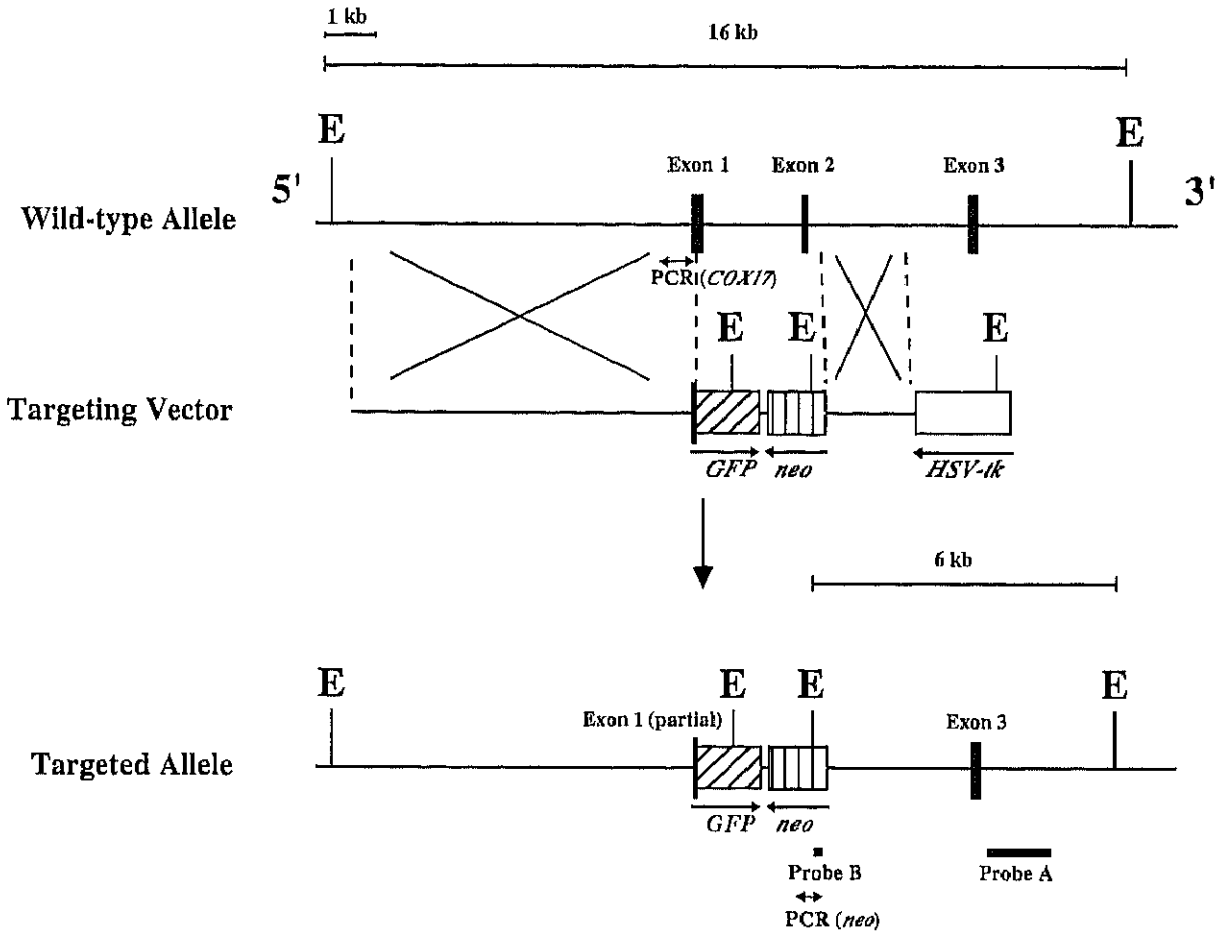

Fig. IV-1. Schematic representation of the targeted disruption of the mouse *COX17* gene. Maps of the wild -type *COX17* allele, the targeting vector, and the targeted *COX17* locus. The solid boxes represent *COX17* exons. A promoter-less GFP gene cassette (hatched box) was inserted 3 bp downstream of the ATG codon of *COX17*. GFP, green fluorescence protein; *neo*, neomycin phosphotransferase; HSV-tk, herpes simplex virus thymidine kinase; and E, *Eco* RI restriction sites. Positions of probes used for genotyping by Southern blot analysis and primers used for genotyping by PCR are indicated, respectively.

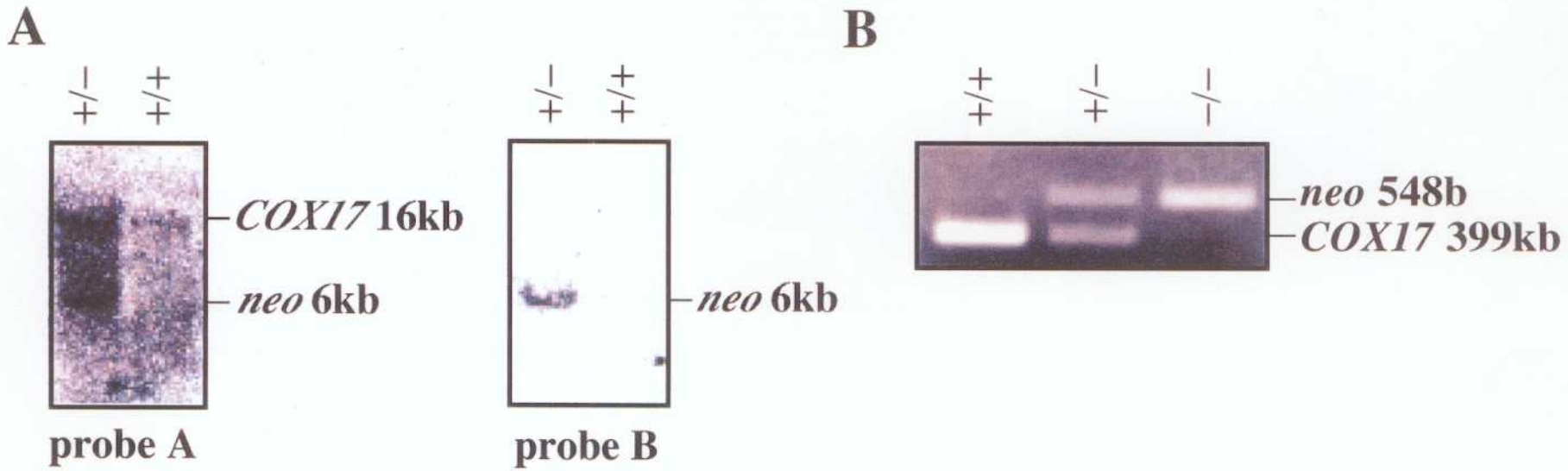

Fig. IV-2. Genotyping analyses of ES cells and E6.5 embryos from heterozygous matings. (A) Southern blot analysis used to screen ES clones and genotype the progeny from heterozygous matings. (B) PCR genotyping of the progeny from heterozygous matings.

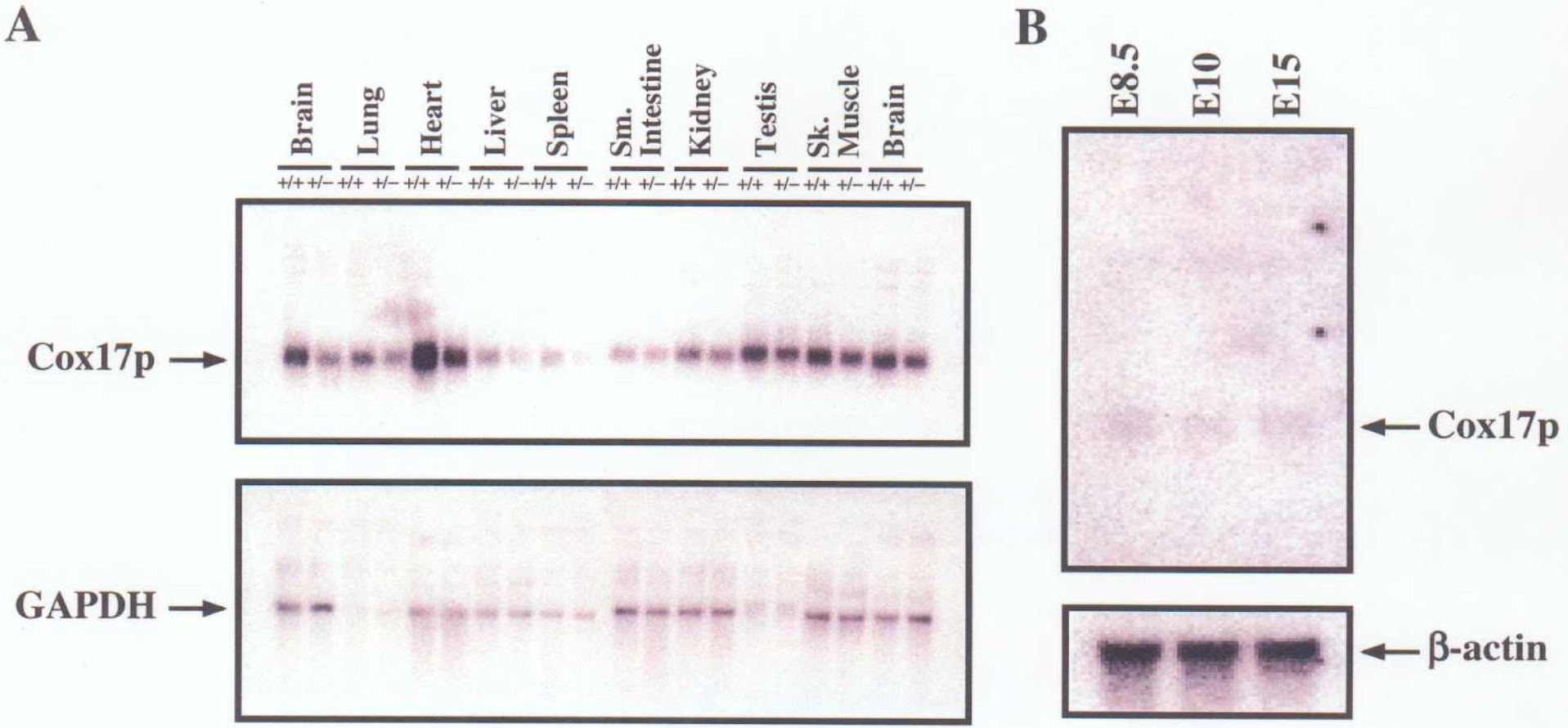

Fig. IV-3. Northern blot analysis of mouse tissues (A) and developmental stages (B) COX17 mRNAs. (A) Analysis of Cox17p mRNA from organs from wild-type and *COX17* (+/-) mice. GAPDH mRNA levels were used as a loading control. (B) Analysis of Cox17p mRNA from E8.5, 10, and 15 embryos. β-actin mRNA levels were used as a loading control.

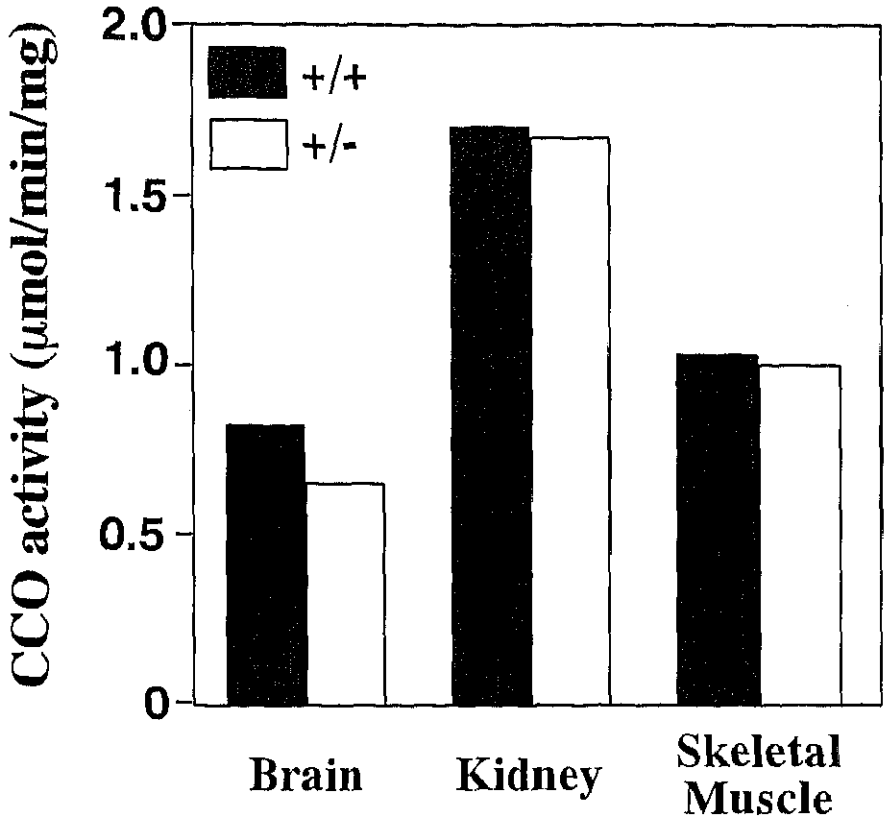

Fig. IV-4. CCO activities in wild-type and *COX17* (+/-) mice. Activities of CCO (μmol/min/mg protein) from whole tissue homogenates were analyzed for 5-6 -week-old wild-type and *COX17* (+/-) littermates. Since CCO activity is slightly reduced in the brains of the heterozygotes compared with wild-type littermates, no significant difference was observed in the kidney or skeletal muscle.

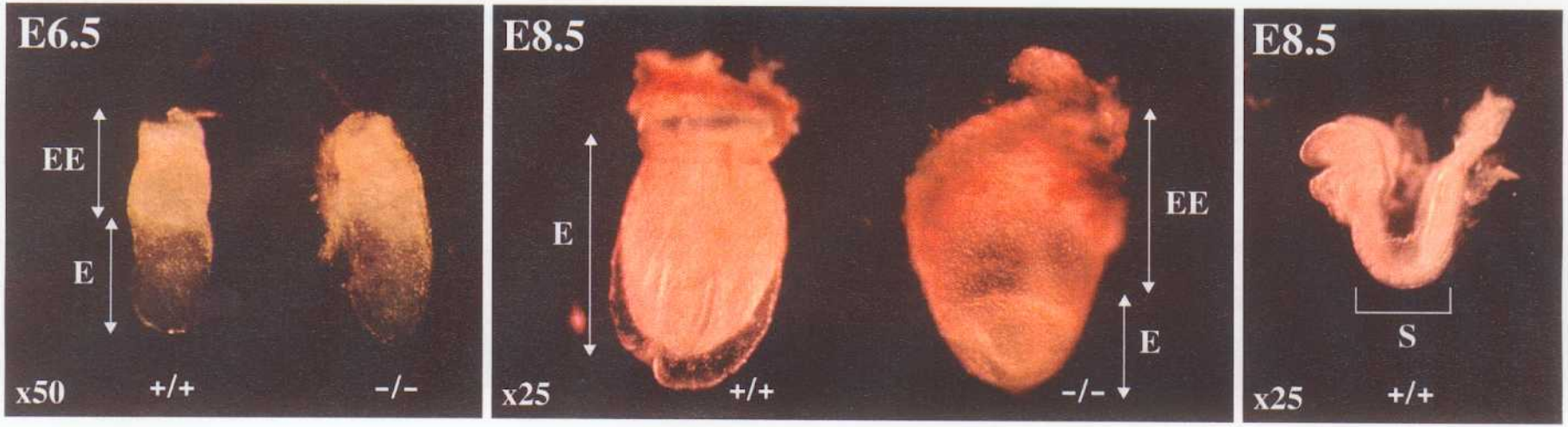

Fig. IV-5. Morphological analysis of wild-type and mutant embryos. Whole-mount gross morphology of wild-type and *COX17* (-/-) embryos at E6.5, and E8.5. The embryos are oriented such that the embryonic region is located at the bottom and the extra-embryonic structures are on the top. All embryos were genotyped by PCR after photography. E, embryonic region; EE, extra-embryonic region; S, somites.

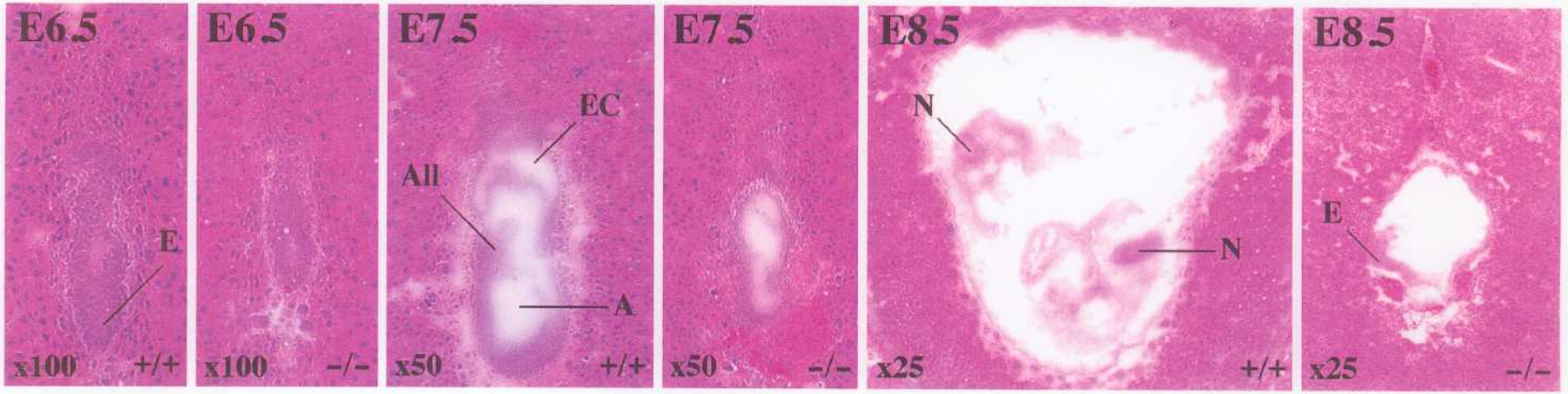

Fig. IV-6. Histological analysis of wild-type and mutant embryos. Hematoxylin and eosin (HE) staining of sagittal sections of wild-type and *COX17* (-/-) E6.5 (x100), E7.5 (x50) and E8.5 (x25) embryos, respectively. A, amniotic cavity; All, allantois; E, embryo; EC, exocoelomic cavity; N, neural tube.

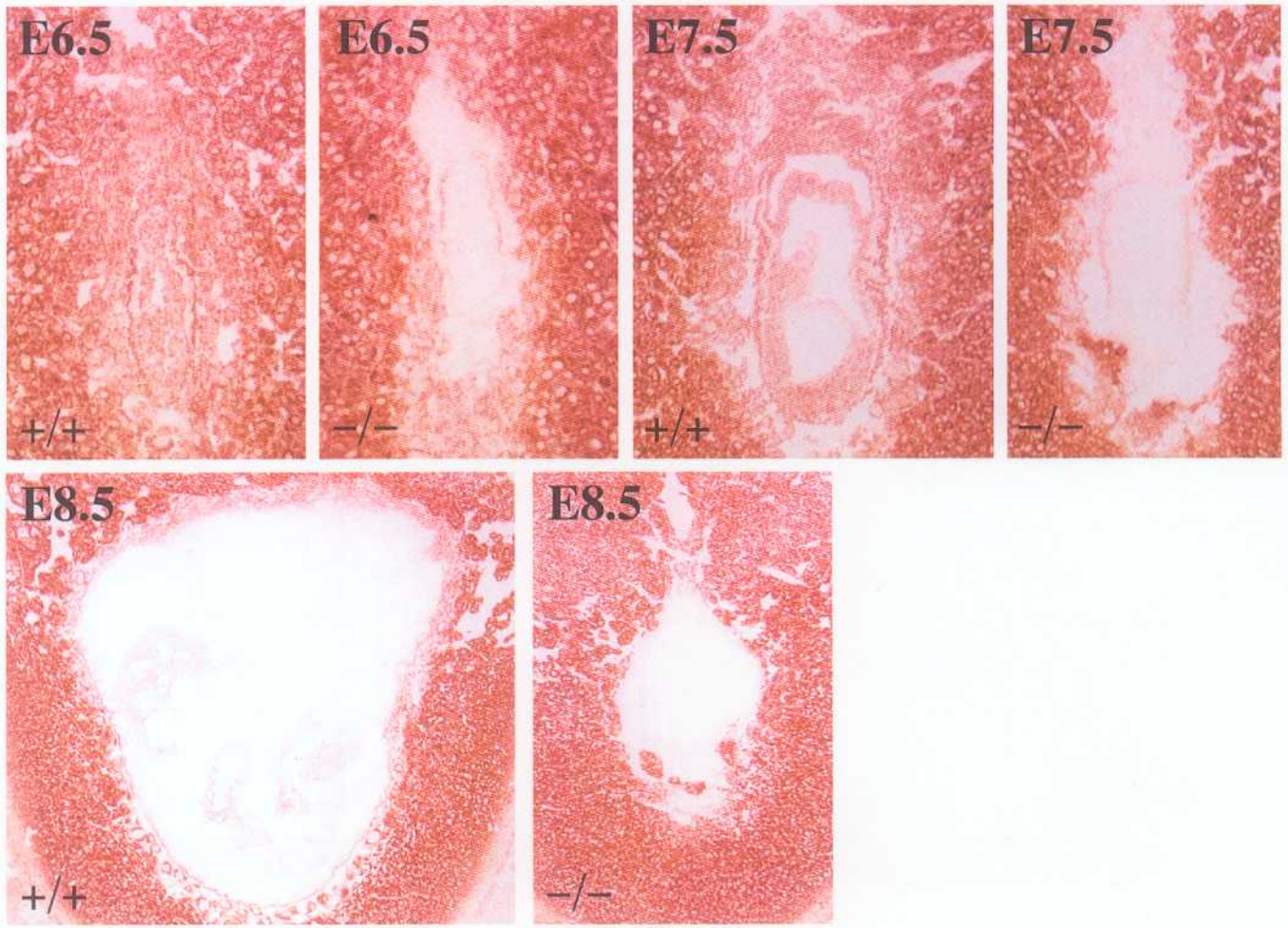

Fig. IV-7. CCO activeties in the wild-type and *COX17*(-/-) embryos at E6.5. Series of sections identical to those shown in Fig. IV-6 and IV-8 were used.

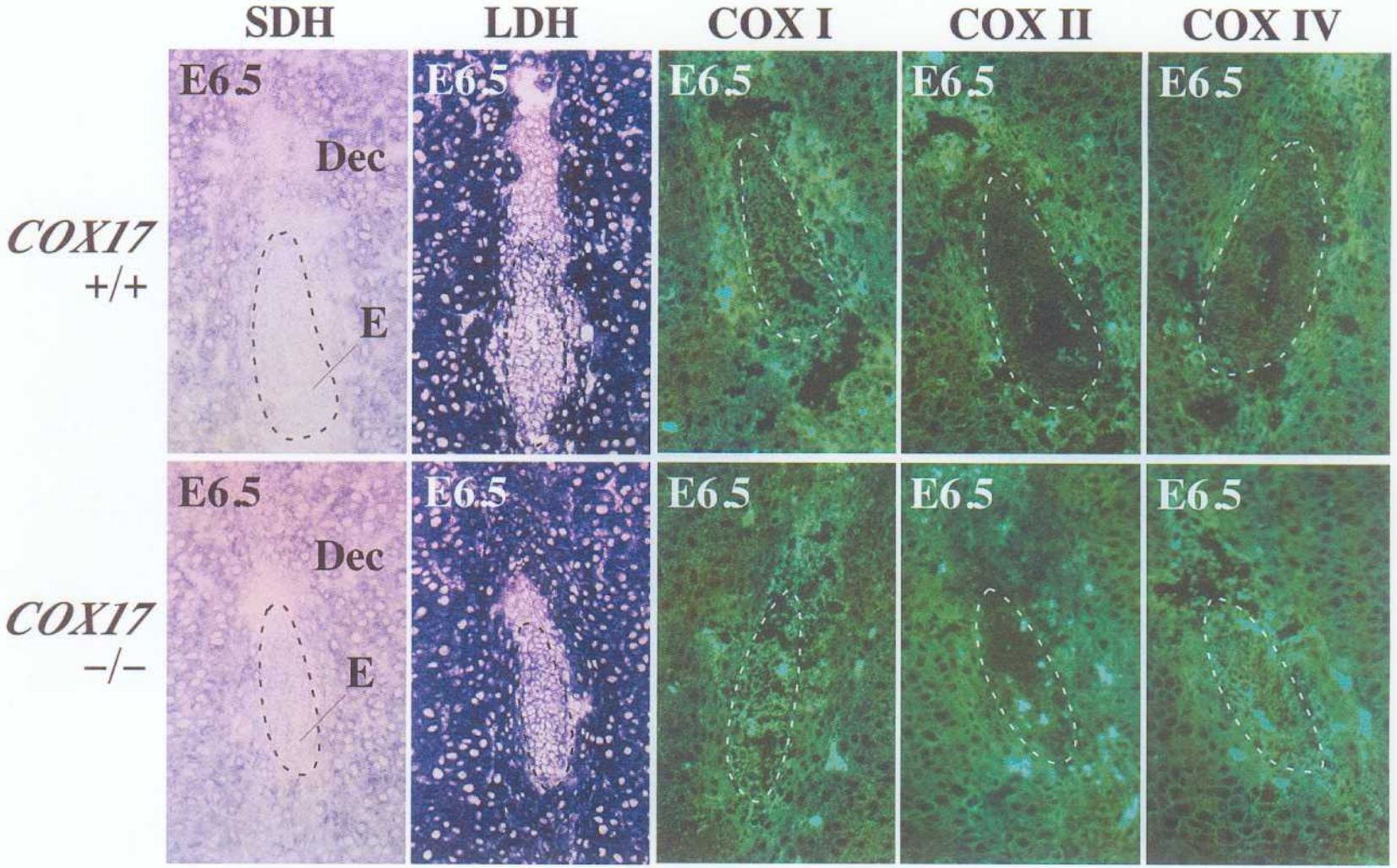

Fig. IV-8. Histochemical examination of sectioned embryos. Activities of SDH and LDH and immunohistochemical staining to detect COX subunits I, II and IV at E6.5 (x100). Series of sections identical to those shown in Fig. IV-6 and IV-7 were used.

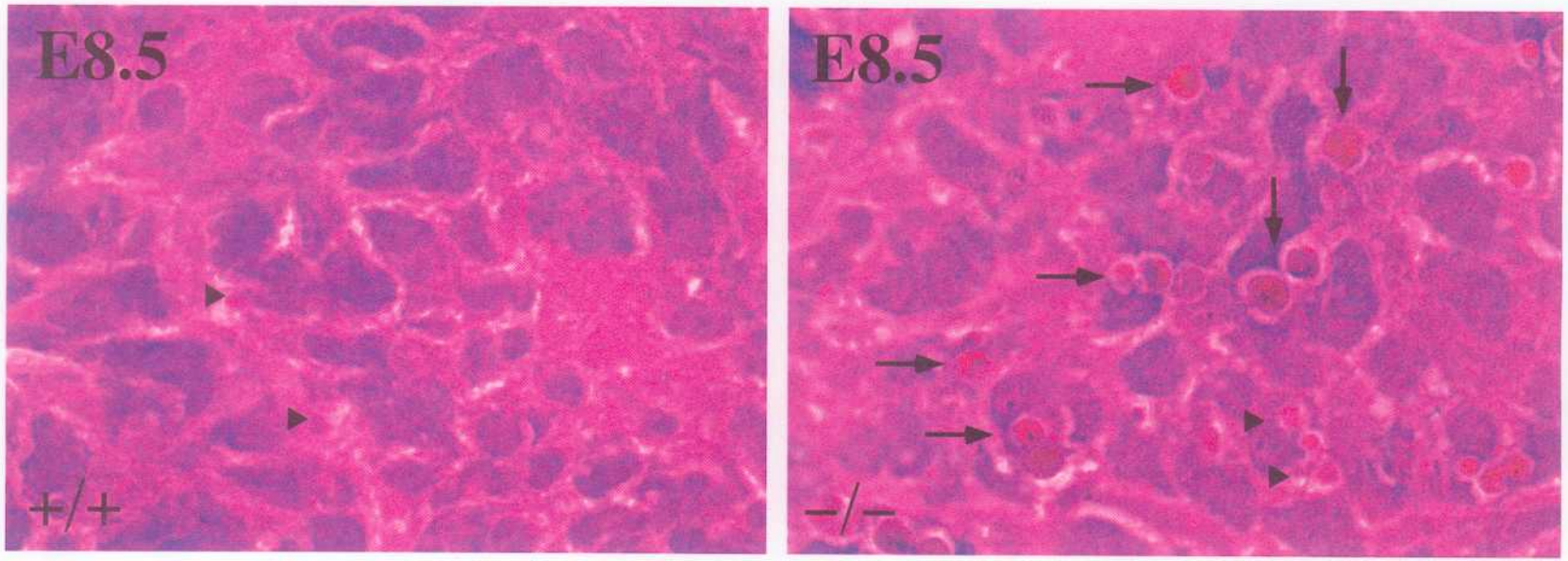

Fig. IV-9. Magnified images of HE staining embryos at E8.5 (x1000) shown in Fig. IV-6. In the mutant embryonic region, many atrophied cells (indicated by arrow head) and nuclear condensation (indicated by arrow) can be seen (right panel). Conversely, in the wild-type embryo, few apoptic cells can be observed (left panel).